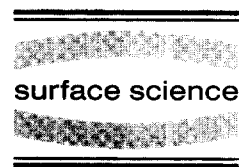




ELSEVIER

Surface Science 370 (1997) L213–L218



Surface Science Letters

## Unique edge structure and stability of fabricated dimer islands on Si(001)

Feng Liu, C.T. Salling, M.G. Lagally \*

*University of Wisconsin, Madison, WI 53706, USA*

Received 6 June 1996; accepted for publication 27 August 1996

---

### Abstract

The edge structure and stability of monolayer-high islands fabricated on Si(001) surfaces by scanning tunneling microscopy have been analyzed theoretically. In contrast to the edges of similar islands grown by depositing Si, the properties of edges of fabricated islands are determined by the length of the trench of dimers that are removed to create the island. We demonstrate the possibility of controlling the edge structure, and thus the stability, through a selective process of atom removal.

*Keywords:* Computer simulations; Silicon; Surface defects; Surface structure; Surface thermodynamics

---

While scanning tunneling microscopy (STM) imaging has advanced remarkably our understanding and knowledge of surface properties and the initial stages of film growth in the last decade, atomic-scale fabrication using the STM is a relatively new frontier. Most recent effort has been devoted to searching for the optimal conditions for atom manipulation. Several different methodologies for forming nanostructures on both metal and semiconductor surfaces have been demonstrated [1–11]. A few studies have also investigated the underlying mechanisms of atom transfer between the STM tip and the sample surface [3,4,12–16]. However, little attention has been paid to the properties of the fabricated structures [9,13].

Confining atoms within nanoscale dimensions

leads to novel electronic and optical properties, presenting promises of future technology as well as new scientific challenges. Technological utility of such nanostructures, however, requires thermal stability under processing and application conditions. These man-made structures are often created far from equilibrium, surviving under peculiar constraints of geometry and local mechanical stress. As a result, structures existing in *artificial* conditions may exhibit stability properties quite different from those of similar structures that occur naturally.

As an example of an artificial structure, consider a monolayer-high island created in a terrace by removal of atoms around it, as shown in Fig. 1. Such an island is identical in orientation and similar in shape to islands formed on a terrace by deposition of Si [17], except that it is surrounded by a “moat” of finite dimension and enclosed by terraces. Using such STM-fabricated monolayer-

---

\*Corresponding author. Fax: +1 608 265 4118;  
e-mail: lagally@engr.wisc.edu

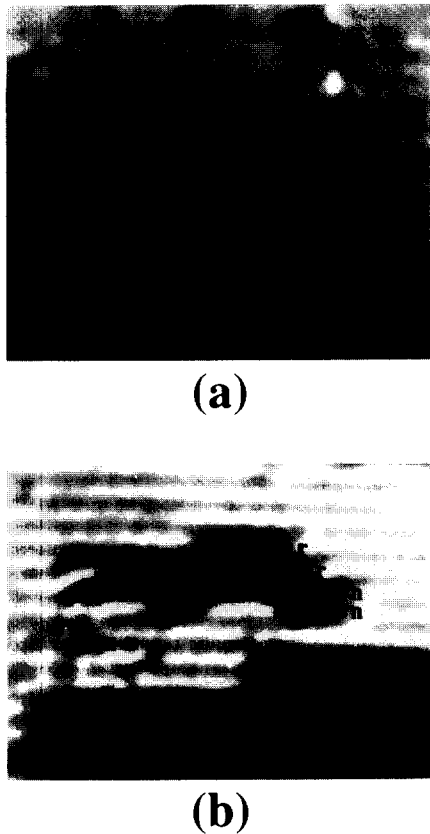


Fig. 1. STM images of fabricated island and trench structures on Si(001). Letters n and r mark the non-rebonded and rebonded  $S_B$  edge, respectively. To identify a rebonded or non-rebonded edge, one looks for the boundary between the bright signal for the upper level atoms and the dimer rows below the step. A rebonded edge ends between two dimer rows below; a non-rebonded edge ends on the top of a dimer row below. Note the presence of all three types of trench terminations (n-r, n-n, and r-r) discussed in the text.

deep structures on Si(001) as model systems, we can study the structural properties and thermal stability of nanopatterned crystalline silicon, and of silicon nanostructures in general.

In this Letter, we discuss the structure of the step edges of such fabricated islands and the consequent stability of the islands. In particular, we show that the structure of the edge in the dimer row direction depends quite naturally on the length of the trench formed in the same row next to the island. We calculate the relative stability of different edge structures and the kinetic barrier for trans-

itions between them. We demonstrate the possibility of fabricating the desirable (i.e. more stable) edge structure through a selective process of atom removal.

We have previously patterned Si(001) surfaces with a STM by transferring atoms from the sample to the STM tip [11]. Si(001) displays a  $(2 \times 1)$  reconstruction consisting of arrays of dimer rows. By tuning to the appropriate conditions, we succeeded in removing a few dimers at a time to create surface structures at room temperature with features that are one atomic layer deep and a few dimers long and wide. We have been able to achieve the removal of as few as two adjacent dimers from a dimer row. The structures shown in Figs. 1a and 1b are typical examples. The atomic configurations in these structures are unchanged at room temperature for the length of time we examined them (several hours). After segments of dimer row are removed to form a monolayer-deep trench, the atoms exposed to the vacuum on the trench floor again dimerize but in the direction orthogonal to the surface dimers because of the tetrahedral bonding configuration in the diamond structure. The trench is bound by two types of monatomic steps, which are also seen on vicinal surfaces. Edges with dimer rows on the upper terrace parallel to the edge are of  $S_A$  type; edges with dimer rows on the upper terrace perpendicular to the edge are of  $S_B$  type [18]. The  $S_B$  edge can have either a rebonded or a non-rebonded configuration [18].

At thermal equilibrium, only rebonded  $S_B$  steps are observed by STM on vicinal surfaces that have been annealed and slowly cooled [19–21]. Experiments [19,21] further show that the  $S_B$  step fluctuates, attaching and detaching two dimers at a time to preserve the rebonded step edges. The observation that the rebonded  $S_B$  step is much more stable than the non-rebonded step is consistent with our calculations (see below). Surprisingly, after examining all the  $S_B$  step edges of our fabricated islands, we find a nearly equal population of rebonded and non-rebonded configurations! To understand this observation, we first recognize that during the fabrication we can create trenches whose length is determined by the removal of an even

number of dimers (which we call an e-trench) and others whose length is determined by removal of an odd number of dimers (an o-trench). By performing a straightforward geometric analysis, using for illustrative purposes a single-dimer wide trench, we demonstrate that the e-trench always produces an equal population of rebonded and non-rebonded  $S_B$  edges, as a mandatory consequence of geometry constraint. The o-trench, on the other hand, geometrically can have either 100% rebonded or 100% non-rebonded edges.

Figs. 2 and 3 illustrate the two possible topologies, respectively, of an e-trench with four missing dimers (Figs. 2b and 2c) and of an o-trench with five missing dimers (Figs. 3b and 3c). Also shown

in the figures are the two transition states (Figs. 2a and 3a) immediately after the surface dimers are removed but before the final trench structures are formed. It is evident that the termination of the trench, in the direction along the dimer row, with either rebonded or non-rebonded  $S_B$  edges is restricted by the geometry constraint. The e-trench must be terminated with a rebonded edge at one end and a non-rebonded edge at the other end; the o-trench must be terminated with two rebonded edges or two non-rebonded edges. Therefore, for the e-trench the asymmetric structure produces a geometric constraint that requires an equal occupation of rebonded and non-rebonded edges, making the energetics an irrelevant factor.

If e-trenches only were created, we would automatically see the same number of rebonded and non-rebonded edges – a possible simple explanation of our observation. However, we have produced o-trenches as well (see Figs. 1a and 1b). In both of them geometrically allowed symmetric structures (same terminations at both ends) appear with almost equal probability. To understand this observation, we have investigated the relative stability of trenches with different terminations. We calculated the trench formation energy as a function of trench length, using an empirical many-body potential [22]. The calculation was performed with a slab sample of 1280 atoms. The surface layer consists of 5 dimer rows, and each row contains 16 dimers. In the actual trench formation process, with atoms being transferred from the sample to the STM tip, there is no unique way to define the trench formation energy, because no knowledge about the final state of those atoms being transferred can be obtained. To simplify the problem, we opt to define the trench formation energy as the energy difference of the fabricated structure before and after the atom transfer event, namely,

$$E_f = E_t^a(N - 2m) - E_t^b(N - 2m). \quad (1)$$

$E_f$  and  $E_t$  denote formation energy and total energy, respectively;  $N$  is the total number of atoms and  $m$  is the number of dimers being removed. The superscripts a and b denote “after” and “before” dimers removal.

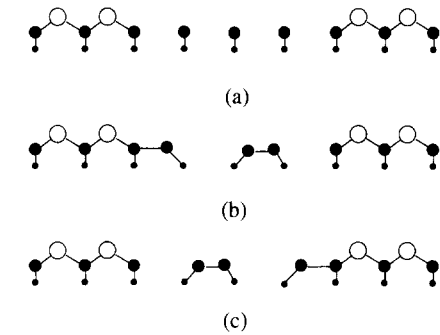


Fig. 2. Schematic side view of an e-trench created by removing four surface layer dimers. (a) Shows the transition state configuration; (b) and (c) show two degenerate final-state configurations, with respectively one rebonded and one non-rebonded edge.

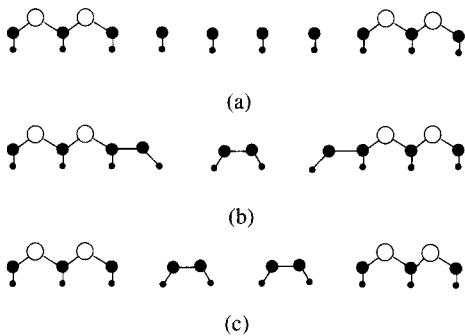


Fig. 3. Schematic side view of an o-trench created by removing five surface layer dimers. (a) Shows the transition state configuration; (b) and (c) show two different final-state configurations with rebonded and non-rebonded  $S_B$  edges, respectively.

In Fig. 4 we plot the trench formation energy against trench length. Three sets of data are plotted: one for an e-trench and one each for an o-trench with rebonded or non-rebonded  $S_B$  edges, respectively. In all three cases, the formation energy increases linearly with trench length. The three lines also have the same slope: it corresponds to the formation energy of two side-by-side  $S_A$  edges in the trench. The o-trench with rebonded  $S_B$  edges is found to be 0.72 eV/dimer more stable than the one with non-rebonded edges (see the constant shift of lines in Fig. 4). We may compare this energy difference with that of rebonded and non-rebonded  $S_B$  steps on a vicinal surface. In calculating the  $S_B$  step energy, we use a 10-layer slab with a  $(2 \times 30)$  surface unit cell. Two  $S_B$  steps on the surface are separated by 15 dimers. We find that the rebonded step is 0.81 eV/dimer more stable than the non-rebonded step. The slightly different result obtained for trench and surface probably reflects the different local strain field in the vicinity of the step edge. The energy gain of 0.72 eV/dimer we obtained for rebonding implies a silicon dangling bond energy of about this magni-

tude, which agrees well with a previous first-principles calculation of the value (1.0 eV/dimer) of the dimerization energy of Si(001) [23]. Earlier empirical tight-binding calculations [18] showed that the rebonded step is *at least* 0.32 eV/dimer more stable than the non-rebonded step but did not put an absolute value on the energy. Using the rebonding energy of 0.72 eV/dimer, we estimate, at room temperature, an equilibrium relative population of  $1 \times 10^{12}$  rebonded edges to 1 non-rebonded edge in o-trenches. We can therefore conclude that the observed structures, which have an approximately equal population of rebonded and non-rebonded edges, must be far from thermal equilibrium. We calculate a large activation barrier (1.0 eV per dimer unit) for transforming an o-trench with non-rebonded edges into an o-trench with rebonded edges. The barrier increases with increasing trench length because a cooperative motion of all the atoms on the trench floor is required. Assuming an attempt frequency of  $10^{13} \text{ s}^{-1}$ , this size of barrier implies an equilibration time of  $10^{30}$  years at room temperature for an o-trench with three missing dimers, excluding other

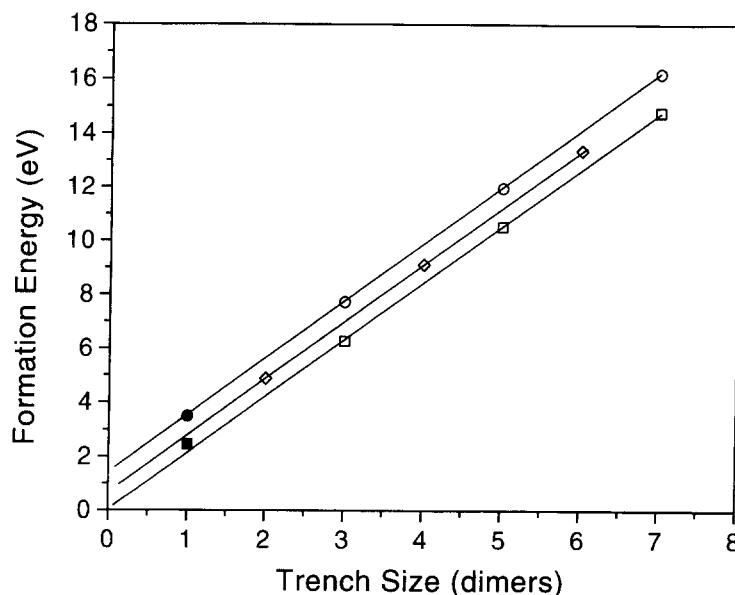


Fig. 4. Trench formation energy as a function of trench length in units of dimers. Open diamonds are the results for e-trenches. Open squares and circles are the results for o-trenches with rebonded and non-rebonded  $S_B$  edges, respectively. Straight lines are the least-square linear fits to the data. The data for a 1-dimer trench (dimer vacancy, solid square and circle) are excluded in the fitting because it has a different bonding configuration.

possible thermal decay processes which may have lower activation barrier (e.g. vacancy formation at the edge).

The extremely high kinetic stability of all possible structural candidates makes the formation process a crucial factor in defining the final rebonded and non-rebonded edge concentrations. In the following, we argue that the chances of forming a rebonded or non-rebonded o-trench is likely to be equal unless the atom removal process is preferentially selected. We limit our discussion here to the o-trench only, because the e-trench has a unique termination combination (one rebonded and one non-rebonded edge) no matter how it is formed. We consider two different o-trench formation processes. In the first, an odd number of dimers is removed from a perfect dimer row; in the second, an odd number of dimers is removed from one end of an existing e-trench. In the first process, the instantaneous transition state of the system, immediately after the surface dimers are removed, consists of the exposed atoms on the trench floor in vertical positions (see Fig. 3a). The exposed atoms will then tilt to either left or right in a correlated way to form a rebonded or non-rebonded termination. It is the randomness of the correlated tilting to left or right that yields the same number of rebonded and non-rebonded o-trenches. The scenario in the second o-trench formation process is quite different. Here, half of the structure is pre-determined. When atoms are removed from one end of an e-trench, the edge configuration at the other end remains intact. Suppose we take one more dimer away from one end of an e-trench with four missing dimers (Figs. 2b or 2c) to form an o-trench with five missing dimers (Figs. 3b or 3c). If we remove this dimer from the rebonded edge of the e-trench, we will end up with an o-trench with non-rebonded edges. If we remove this dimer from the non-rebonded edge of the e-trench, we will end up with an o-trench with rebonded edges. The final o-trench configuration therefore depends on the end from which an odd number of dimers is removed. This analysis suggests a clear way to fabricate desirable structures through selective removal. Because we were not yet aware of this possibility [11], we

removed atoms from either end randomly, which led to the observed overall equal average of rebonded and non-rebonded o-trenches.

So far, we have discussed the topology of the edges of fabricated monolayer-high islands in terms of geometric constraints produced by the trench length. We have calculated the kinetic stability of trench structures within a limited context, i.e. without mass transport and defect formation. The fabricated island structures, however, can thermally decay by lateral adsorption and desorption or by defect formation. These processes may occur with lower activation barriers than we have determined above. The lifetime of a fabricated structure is determined by the decay route with the lowest activation barrier. Previously, we had adopted the activation barrier for atom attachment and detachment at a  $S_B$  step to estimate the lifetime of trench structures and other structures containing  $S_B$  edges [11]. A lifetime of about 100 years at room temperature but only 10 ms at 325°C was obtained using an activation barrier of 1.5 eV [19,21]. This earlier analysis is likely to be incorrect. For the sake of simplicity, we will only consider atomic diffusion along the dimer row on Si(001) [17] to analyze the kinetics of atom attachment and detachment at  $S_B$  step edges. On vicinal surfaces atoms can come to and leave an  $S_B$  step, diffusing along dimer rows on the upper terrace. Also, atoms can change and exchange their positions along the step edge, diffusing along the dimer row next to the step edge on the lower terrace. Both processes contribute to the kinetics of atom attachment and detachment at an  $S_B$  step. However, the freedom of atomic movement around a trench structure is limited by the geometry constraint. Atoms can only approach and leave the  $S_B$  edges in the trench through diffusion on the upper terrace, while diffusion on the lower terrace (inside the trench) is forbidden. Therefore, it is inappropriate to apply the energy parameters of an  $S_B$  step on vicinal surfaces to an analysis of the kinetic stability of an  $S_B$  edge in surface trenches, because different kinetic processes are involved. Although the detailed mechanism of atom attachment and detachment at an  $S_B$  step on vicinal surfaces or at an  $S_B$  edge in surface trenches is still unknown [19,21], we speculate that the  $S_B$  edges in surface trenches are kinetically more stable against mass transport and

defect migration than the  $S_B$  steps on vicinal surfaces because of the additional geometric constraints on atomic motion in surface trenches.

In summary, we have shown that several different factors, the geometric constraints, the kinetic stability and the formation process act in concert to make the  $S_B$  edge structure and stability of fabricated islands differ from those of islands grown by deposition on vicinal surfaces. For island edges separated by an e-trench along the dimer row direction, the equal population of rebonded and non-rebonded edges is an intrinsic geometric property of the e-trench. For island edges separated by an o-trench, our calculations show that the rebonded edges are more stable than the non-rebonded ones by 0.72 eV/dimer. However, the two states are separated by a very large trench-length-dependent kinetic barrier, so the probability of conversion at room temperature from the non-rebonded into the rebonded configuration is negligible. As a result, the equal chance of forming the two configurations during the STM fabrication leads to an overall nearly equal population of rebonded and non-rebonded edges. We have also shown that it is possible to manipulate the edge configuration of an island by choosing carefully the removal process and trench length.

### Acknowledgements

We acknowledge helpful discussions with N. Kitamura. This work was supported by AFOSR.

### References

- [1] R.S. Becker, J.A. Golovchenko and B.S. Swartzentruber, *Nature* 325 (1987) 419.
- [2] R.M. Silver, E.E. Ehrichs and A.L. de Lozanne, *Appl. Phys. Lett.* 51 (1987) 247.
- [3] M.A. McCord and R.F.W. Pease, *J. Vac. Sci. Technol. B* 5 (1987) 430.
- [4] J.A. Dagata, J. Schneir, H.H. Harary, C.J. Evans, M.T. Postek and J. Bennett, *Appl. Phys. Lett.* 56 (1990) 2001.
- [5] J.A. Stroscio and D.M. Eigler, *Science* 254 (1991) 1319.
- [6] H.J. Mamin, S. Chiang, H. Birk, P.H. Guethner and D. Rugar, *J. Vac. Sci. Technol. B* 9 (1991) 1398.
- [7] S. Hosoki, S. Hosaka and T. Hasegawa, *Appl. Surf. Sci.* 60/61 (1992) 643.
- [8] W. Li, J.A. Virtanen and R.M. Penner, *Appl. Phys. Lett.* 60 (1992) 1181.
- [9] M.F. Crommie, C.P. Lutz and D.M. Eigler, *Science* 262 (1993) 218.
- [10] M. Aono, A. Kobayashi, F. Grey, H. Uchida and D. Huang, *Jpn. J. Appl. Phys.* 32 (1993) 1470.
- [11] C.T. Salling and M.G. Lagally, *Science* 265 (1994) 502.
- [12] N.D. Lang, *Phys. Rev. B* 45 (1992) 13599.
- [13] I.-W. Lyo and Ph. Avouris, *Science* 253 (1990) 173.
- [14] A. Kobayashi, F. Grey, R.S. Williams and M. Aono, *Science* 259 (1993) 1724.
- [15] Y. Hasegawa and Ph. Avouris, *Science* 258 (1992) 1763.
- [16] T.T. Tsong, *Phys. Rev. Lett.* 72 (1994) 574.
- [17] Y.W. Mo, B.S. Swartzentruber, R. Kariotis, M.B. Webb and M.G. Lagally, *Phys. Rev. Lett.* 63 (1989) 2393; Y.W. Mo, J. Kleiner, M.B. Webb and M.G. Lagally, *Phys. Rev. Lett.* 66 (1991) 1998.
- [18] J.D. Chadi, *Phys. Rev. Lett.* 59 (1987) 1691.
- [19] N. Kitamura, B.S. Swartzentruber, M.G. Lagally and M.B. Webb, *Phys. Rev. B* 48 (1993) 5704.
- [20] Fang Wu, personal communication.
- [21] B.S. Swartzentruber and M. Schacht, *Surf. Sci.* 322 (1995) 83.
- [22] J. Tersoff, *Phys. Rev. B* 39 (1989) 5566.
- [23] N. Roberts and R.J. Needs, *Surf. Sci.* 236 (1990) 112.